APPLIED AND ENVIRONMENTAL MICROBIOLOGY, Apr. 2004, p. 2211–2219 Vol. 70, No. 4
0099-2240/04/$08.00+0 DOI: 10.1128/AEM.70.4.2211–2219.2004

Phenol Hydroxylase and Toluene/*o*-Xylene Monooxygenase from *Pseudomonas stutzeri* OX1: Interplay between Two Enzymes

Valeria Cafaro,[1]† Viviana Izzo,[1]† Roberta Scognamiglio,[1]† Eugenio Notomista,[1] Paola Capasso,[1] Annarita Casbarra,[2] Piero Pucci,[2] and Alberto Di Donato[1]*

Dipartimento di Chimica Biologica, Università di Napoli Federico II, 16-80134 Naples,[1] and Dipartimento di Chimica Organica e Biochimica, Università di Napoli Federico II, 45-80126 Naples,[2] Italy

Received 26 August 2003/Accepted 9 January 2004

Degradation of aromatic hydrocarbons by aerobic bacteria is generally divided into an upper pathway, which produces dihydroxylated aromatic intermediates by the action of monooxygenases, and a lower pathway, which processes these intermediates down to molecules that enter the citric acid cycle. Bacterial multicomponent monooxygenases (BMMs) are a family of enzymes divided into six distinct groups. Most bacterial genomes code for only one BMM, but a few cases (3 out of 31) of genomes coding for more than a single monooxygenase have been found. One such case is the genome of *Pseudomonas stutzeri* OX1, in which two different monooxygenases have been found, phenol hydroxylase (PH) and toluene/*o*-xylene monooxygenase (ToMO). We have already demonstrated that ToMO is an oligomeric protein whose subunits transfer electrons from NADH to oxygen, which is eventually incorporated into the aromatic substrate. However, no molecular data are available on the structure and on the mechanism of action of PH. To understand the metabolic significance of the association of two similar enzymatic activities in the same microorganism, we expressed and characterized this novel phenol hydroxylase. Our data indicate that the PH P component of PH transfers electrons from NADH to a subcomplex endowed with hydroxylase activity. Moreover, a regulatory function can be suggested for subunit PH M. Data on the specificity and the kinetic constants of ToMO and PH strongly support the hypothesis that coupling between the two enzymatic systems optimizes the use of nonhydroxylated aromatic molecules by the draining effect of PH on the product(s) of oxidation catalyzed by ToMO, thus avoiding phenol accumulation.

Aerobic bacterial degradation of aromatic hydrocarbons is generally divided into two major routes (1, 13), the so-called upper pathway, which leads to the formation of partially oxidized aromatic intermediates, and a lower pathway, which uses dihydroxylated aromatic molecules. These activated aromatic compounds undergo ring cleavage reactions and are further processed to give molecules that can eventually enter the citric acid cycle.

Monooxygenases are key enzymes in the upper pathway and catalyze hydroxylation of the aromatic ring at different positions (22, 33, 37). Recently (21), it has been recognized that bacterial multicomponent monooxygenases (BMMs) constitute a family of enzymes which can be divided into six distinct groups, each with a characteristic subunit composition. BMMs are transcribed from single operons that code for four to six polypeptides. Analysis of the sequences from nucleotide and protein databases indicates that most bacterial strains possess only one BMM, but a few cases (3 out of 31) of bacterial genomes coding for more than one monooxygenase have been found (21). Two group 1 (phenol hydroxylases) and one group 2 (toluene-benzene monooxygenases) BMMs have been found in the genome of *Ralstonia metallidurans* CH34 (21), and three BMMs belonging to groups 1 and 2 were detected in *Burkholderia cepacia* (formerly *Pseudomonas cepacia*) JS150 (16, 21). *B. cepacia* JS150 instead is endowed with the ability to use different pathways for the metabolism of substituted aromatic compounds (16). This led to the suggestion that in *B. cepacia* JS150, toluene metabolism is initiated by one dioxygenase and two distinct BMMs with different specificities (a toluene 4-monooxygenase [T4MO] belonging to group 2 and a toluene 2-monooxygenase [T2MO] belonging to group 1), whereas a third BMM acts downstream of the other two monooxygenases (16).

Pseudomonas stutzeri OX1 is able to grow on a wide spectrum of aromatics, including phenol, cresols, and dimethylphenols, but also on nonhydroxylated molecules such as toluene, *o*-xylene (2, 3), and benzene (P. Barbieri, personal communication). Two different monooxygenases have been found in the genome of *P. stutzeri* OX1, phenol hydroxylase (PH) (1) and toluene *o*-xylene monooxygenase (ToMO) (3, 4).

ToMO is endowed with a broad spectrum of substrate specificity and with the ability to hydroxylate more than a single position of the aromatic ring in two consecutive monooxygenation reactions (3). Thus, ToMO is able to oxidize *o*-, *m*-, and *p*-xylene, 2,3- and 3,4-dimethylphenol, toluene, cresols, benzene, naphthalene, and styrene (3). Moreover, ethylbenzene (3), trichloroethylene, 1,1-dichloroethylene, chloroform (7), and tetrachloroethylene (29) can also be oxidized by the enzyme.

Recombinant ToMO has recently been expressed and reconstituted in vitro (6). It has been shown that ToMO is an

* Corresponding author. Mailing address: Dipartimento di Chimica Biologica, Università di Napoli Federico II, Via Mezzocannone, 16-80134 Naples, Italy. Phone: 39 81 674171. Fax: 39 81 676710. E-mail: didonato@unina.it.

† Valeria Cafaro, Viviana Izzo, and Roberta Scognamiglio contributed equally to this work.

oligomeric protein whose subunits are part of an electron transfer chain in which ToMO F, an NADH-oxidoreductase, transfers electrons from NADH to ToMO C, which is a Rieske-type ferredoxin that shifts electrons to the oxygenase ToMO H component, made up of the ToMO A, B, and E subunits. Another subunit of the complex is ToMO D, for which a regulatory function has been suggested (4, 31).

Two kilobases downstream of the gene cluster coding for ToMO, another cluster coding for a phenol hydroxylase was found (1). Southern hybridization analyses with the *dmp* genes, coding for the subunits of the *Pseudomonas* sp. strain CF600 multicomponent phenol hydroxylase, gave evidence that the *P. stutzeri* cluster is homologous to that of *Pseudomonas* sp. strain CF600 (1). This suggests that the *P. stutzeri* OX1 phenol hydroxylase is a multicomponent enzyme. Moreover, activity assays carried out on recombinant *Escherichia coli* cells harboring cloned phenol hydroxylase showed that the cells express an enzymatic activity that is able to hydroxylate not only phenol but also 2,4-dimethylphenol and 2,5-dimethylphenol (1). Thus, it seems that in the case of *P. stutzeri* OX1, an association of BMMs is also present and that the two BMMs have similar substrate specificities.

To shed light on the metabolic significance of the copresence of two similar enzymatic activities in the same microorganism, we expressed and characterized the novel phenol hydroxylase from *P. stutzeri* and collected data on the specificity and the kinetic constants of the two different monooxygenases. Our data support the hypothesis that coupling between the two enzymatic systems optimizes the use of nonhydroxylated aromatic molecules by the draining effect of PH on the product(s) of oxidation catalyzed by ToMO, thus avoiding phenol accumulation.

MATERIALS AND METHODS

Materials. Bacterial cultures, plasmid purifications and transformations were performed according to Sambrook et al. (30). The pET22b(+) expression vector and *E. coli* strains BL21(DE3) and JM109 were from Novagen, whereas *E. coli* strain JM101 was purchased from Boehringer. The thermostable recombinant DNA polymerase used for PCR amplification was Platinum *Pfx* from Life Technologies, and deoxynucleotide triphosphates were purchased from Perkin-Elmer Cetus. The Wizard PCR Preps DNA purification system for elution of DNA fragments from agarose gels was obtained from Promega. Enzymes and other reagents for DNA manipulation were from New England Biolabs. The oligonucleotides were synthesized at the Stazione Zoologica A. Dohrn (Naples, Italy). Polyvinylidene difluoride membranes were from Perkin Elmer Cetus. Protease inhibitor cocktail EDTA-free tablets were purchased from Boehringer. Superose 12 PC 3.2/30, Q-Sepharose Fast Flow, Sephacryl S300 High Resolution, Sephadex G75 Superfine, and disposable PD10 desalting columns were from Pharmacia. CNBr was from Pierce, and cytochrome *c* from horse heart, trypsin, endoproteinase LysC, and bovine insulin were from Sigma. All other chemicals were from Sigma. The expression and purification of catechol 2,3-dioxygenase from *P. stutzeri* OX1 will be described in another paper (A. Viggiani, unpublished data).

Nucleotide sequencing. DNA fragments were directly sequenced by the walking-primer method with an automated sequencer (ABI 3100, Applied Biosystems, Foster City, Calif.) with the ABI Prism Big-Dye terminator cycle sequencing ready reaction kit (Applied Biosystems).

Construction of expression vectors. Plasmids pBZ1260 (3) and pJSX148 (1), containing ToMO and PH gene clusters, respectively, were kindly supplied by P. Barbieri (Dipartimento di Biologia Strutturale e Funzionale, Università dell'Insubria, Varese, Italy). The DNA sequences coding for subunits PH P and PH M from plasmid pJSX148 were subcloned into vector pET22b(+) with a PCR procedure to insert the appropriate endonuclease restriction sites at the 5′ and 3′ ends of each gene to allow their polar cloning into the expression vector, with synthetic oligonucleotides specific for each gene. Primers *PHPup* (5′-CCGGAATTCATATGAGTTACACCGTC-3′) and *PHPdown* (5′-CCCAAGCTTCTATATCTTCTTGAACA-3′) were used for the amplification of a 1,062-bp fragment containing the *ph p* gene, coding for PH P. Primers *PHMup* (5′-CCGGAATTCATATGAGCCAGCTTGTAT-3′) and *PHMdown* (5′-CCCAAGCTTAATTCCATTCAAGAATG-3′) were used for the amplification of a 267-bp fragment containing the *ph m* gene, coding for PH M. Primers *PHPup* and *PHMup* introduced an NdeI restriction site at the *ph p* and *ph m* ATG start codons, whereas primers *PHPdown* and *PHMdown* inserted a HindIII restriction site downstream of the stop codons of both genes. The DNA fragments coding for PH P and PH M from the PCR amplifications were isolated by agarose gel electrophoresis, eluted, and digested with NdeI and HindIII restriction endonucleases. The digestion products were purified by electrophoresis, ligated with pET22b(+) previously cut with NdeI and HindIII, and used to transform JM101 competent cells. The resulting recombinant plasmids, named pET22b(+)/phP and pET22b(+)/phM, respectively, were verified by DNA sequencing.

Expression and purification of the PH complex and of subunits PH P and PH M. Plasmid pJSX148 and plasmid pBZ1260, containing the *ph* and *tou* (genetic locus for the ToMO complex) gene clusters, respectively, were expressed in *E. coli* JM109 cells. Plasmids pET22b(+)/phP and pET22b(+)/phM were expressed in *E. coli* BL21(DE3) cells.

All recombinant strains were routinely grown in Luria-Bertani (LB) medium (30) supplemented with 50 μg of ampicillin per ml. Fresh transformed cells were inoculated into 10 ml of LB-ampicillin medium at 37°C, up to an optical density at 600 nm (OD_{600}) of 0.7. These cultures were used to inoculate 1 liter of LB supplemented with 50 μg of ampicillin per ml and grown at 37°C until the A_{600} ranged from 0.7 to 0.8.

Expression of recombinant proteins was induced by adding isopropylthiogalactopyranoside (IPTG) at a final concentration of 70 μM for pET22b(+)/phP, 0.4 mM for pET22b(+)/phM, and 0.4 mM for the expression of the *ph* gene cluster from plasmid pJSX148. At the time of induction, $Fe(NH_4)_2(SO_4)_2$ was added at a final concentration of 100 μM except in the case of PH M. Growth was continued for 3 h at 37°C for expression of the PH complex and at 25°C in the case of pET22b(+)/phP and pET22b(+)/phM. Cells were collected by centrifugation, washed in 25 mM MOPS (morpholinopropanesulfonic acid, pH 6.9) containing 10% ethanol, 10% glycerol, and 1 mM dithiothreitol (buffer A) or in 20 mM sodium phosphate (pH 7.0)–10% glycerol (buffer B). The cell paste was stored at −80°C until needed.

An sodium dodecyl sulfate-polyacrylamide gel electrophoresis (SDS-PAGE) analysis of an aliquot of induced and noninduced cells, after sonication and separation of the soluble and insoluble fractions, revealed that, based on the expected molecular sizes of the polypeptides, all the proteins of interest were present only in the soluble fraction of the induced cells. Typical yields, on the basis of densitometric scanning of the electrophoresis profiles obtained after cell lysis, were approximately 40 mg/liter for PH P, 28 mg/liter for PH M, and 10 mg/liter for PH LNO. The paste from 1 liter of culture of induced cells was suspended in 40 ml of the appropriate buffer containing an EDTA-free protease inhibitor cocktail. Cells were disrupted by sonication (10 times for a 1-min cycle, on ice). Cell debris was removed by centrifugation at 18,000 × *g* for 60 min at 4°C. The supernatant was immediately fractionated as described below. Unless otherwise stated, all chromatographic steps were performed at 4°C. Buffers were made anaerobic by repeated cycles of flushing with nitrogen. Column operations were not strictly anoxic.

Purification of the expression products of pJSX148. The soluble fraction from a 1-liter culture of JM109 cells expressing plasmid pJSX148 was loaded onto a Q-Sepharose Fast Flow column (1 by 18 cm) equilibrated in buffer A at a flow rate of 10 ml/h. The column was further washed with 30 ml of the same buffer. Elution was performed with a 200-ml linear salt gradient from 0.08 to 1 M NaCl in buffer A, at a flow rate of 10 ml/h. SDS gel electrophoresis of the fractions eluted from the column (data not shown) indicated that fractions eluting at about 0.4 M NaCl contained three polypeptides with apparent molecular masses of about 10, 38, and 60 kDa, the expected molecular sizes of recombinant subunits O, L, and N, respectively. The identity of the proteins was further checked by N-terminal sequencing of the electrophoresis bands electroblotted onto polyvinylidene difluoride membranes (17). Relevant fractions were pooled, concentrated by ultrafiltration on an XM50 membrane, and loaded onto a Sephacryl S300 High Resolution column (2.5 by 50 cm) equilibrated in buffer A containing 0.2 M NaCl, at a flow rate of 8 ml/h. SDS-PAGE analysis of the fractions (Fig. 1) showed that PH O, N, and L coeluted in a single peak. Fractions were pooled, concentrated by ultrafiltration on XM50, and stored under nitrogen at −80°C.

Purification of PH P. The soluble fraction from a 1-liter culture of cells expressing plasmid pET22b(+)/phP was loaded onto a Q-Sepharose Fast Flow column (1 by 18 cm) equilibrated in buffer B containing 0.08 M NaCl and 1 mM dithiothreitol, at a flow rate of 10 ml/h, and further washed with 30 ml of the

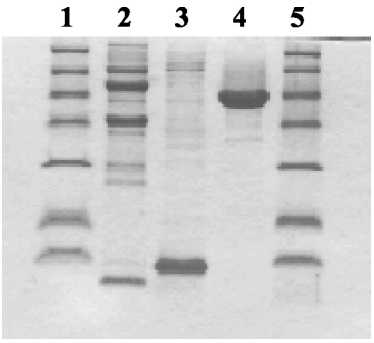

FIG. 1. SDS-PAGE analysis of purified PH subunits. Lanes 1 and 5, molecular mass standards (β-galactosidase, 116.0 kDa; bovine serum albumin, 66.2 kDa; ovalbumin, 45.0 kDa; lactate dehydrogenase, 35.0 kDa; restriction endonuclease Bsp981, 25.0 kDa; β-lactoglobulin, 18.4 kDa; lysozyme, 14.4 kDa). Lane 2, PH (LNO) (2.58 μg); lane 3, PH M (2.22 μg); lane 4, PH P (4.34 μg).

same buffer. Proteins were eluted with a 200-ml linear salt gradient from 0.15 to 0.55 M NaCl, at a flow rate of 10 ml/h. Fractions eluting at about 0.37 M NaCl were found to contain PH P, based on their UV/visible light absorption at 280 and 460 nm, SDS-PAGE analysis, and N-terminal sequencing of the electrophoresis band electroblotted onto polyvinylidene difluoride membranes (17). Relevant fractions were pooled, concentrated by ultrafiltration on YM30 membranes, and loaded onto a Sephadex G75 Superfine column (2.5 by 50 cm) equilibrated in buffer B containing 0.2 M NaCl and 1 mM dithiothreitol, at a flow rate of 8 ml/h. Fractions containing electrophoretically pure PH P (Fig. 1) were pooled, purged with N_2, concentrated by ultrafiltration on YM30 membranes, and stored at −80°C.

Purification of PH M. The soluble fraction from a 1-liter culture of cells expressing plasmid pET22b(+)/phM was loaded onto a Q-Sepharose Fast Flow column (1 by 18 cm) equilibrated in buffer B at a flow rate of 10 ml/h, and the column was further washed with 30 ml of the same buffer. Proteins were eluted with a 200-ml linear salt gradient from 0 to 0.5 M NaCl in buffer B, at a flow rate of 10 ml/h. Fractions eluting at about 0.3 M NaCl were found to contain PH M, based on SDS-PAGE analysis and N-terminal sequencing of the electrophoresis band electroblotted onto polyvinylidene difluoride membranes (17). Relevant fractions were pooled, concentrated by ultrafiltration on YM10 membrane, and loaded onto a Sephadex G75 Superfine column (2.5 by 50 cm) equilibrated in buffer B containing 0.2 M NaCl, at a flow rate of 8 ml/h. Fractions containing electrophoretically pure PH M (Fig. 1) were pooled, purged with N_2, concentrated by ultrafiltration on YM10 membranes, and stored at −80°C.

Primary structure determinations. The primary structure of recombinant subunits was verified by the peptide mapping strategy (6). Aliquots of the high-pressure liquid chromatography (HPLC) product of each purified protein were digested with trypsin and/or endoproteinase LysC and BrCN, and the resulting peptide mixtures were analyzed by matrix-assisted laser desorption ionization-time of flight (MALDI-TOF)/mass spectrometry (MS). The mass signals recorded in the spectra were mapped onto the anticipated sequence of the subunit on the basis of their mass values and the specificity of the enzyme used, leading to verification of the amino acid sequence.

Catalytic assays of reconstituted PH and PH subunits. The enzymatic activity of the reconstituted PH complex was measured on phenol as a substrate by monitoring the production of catechol in continuous coupled assays with recombinant catechol 2,3-dioxygenase from *P. stutzeri* OX1 as already described (6). Protein concentrations were 0.143, 0.201, and 0.849 μM for PH LNO, PH P, and PH M, respectively. Semialdehyde amounts produced from catechol were determined by measuring the absorbance at 410 nm, with an extinction coefficient of 17,300 M^{-1} cm^{-1}. Specific activity was defined as nanomoles of substrate converted per minute per milligram of subcomplex (LNO) at 25°C.

Single-turnover assays of purified components of the PH complex [5.35 nmol of $(LNO)_2$, 14 nmol of PH M, and 12.25 nmol of PH P] and of all of their possible combinations were also performed as already described (6).

The reductase activity of PH P was assayed spectrophotometrically at 25°C by monitoring the reduction of cytochrome *c* at 550 nm with a Cary 100 WinUV Varian spectrophotometer. Assays were carried out as described (32), 1 U of enzymatic activity being defined as the amount of enzyme catalyzing the reduction of 1 μmol of cytochrome *c* per min under the assay conditions. Kinetic parameters for NADH and NADPH were determined with 1.5 nM PH P and 30 μM horse heart cytochrome *c* in the presence of various concentrations of the cofactors.

Enzymatic assays on cells. (i) Enzymatic assays on phenol. Assays were performed with *E. coli* JM109 cells transformed with plasmid pJSX148 or pBZ1260, expressing PH and ToMO, respectively. Cells were grown in LB containing 50 μg of ampicillin per ml at 37°C, up to an OD_{600} of 0.5. Expression of recombinant complexes was induced with 0.4 mM IPTG at 37°C in the presence of 100 μM $Fe(NH_4)_2(SO_4)_2$. One hour after induction, cells were collected by centrifugation and suspended in M9 minimal medium containing 0.4% glucose (M9-G). The specific activity of cells on phenol was determined by their incubation at an OD_{600} of 0.1 to 0.5 in a quartz cuvette in a final volume of 500 μl of M9-G, 400 μM phenol, and saturating amounts of catechol 2,3-dioxygenase (C2,3O) (3 U). The rate of formation of catechol (ε_{375} = 29,100 M^{-1} cm^{-1}) was measured at 375 nm and 25°C. The specific activity of cells ranged between 4 and 6 mU/OD_{600} for cells expressing the PH complex and 15 to 20 mU/OD_{600} for cells expressing the ToMO complex, 1 mU representing 1 nmol of phenol oxidized per min at 25°C.

For determination of the kinetic parameters on phenol, cells were used at an optical density corresponding to 0.3 mU/ml.

(ii) Enzymatic assays on benzene. Activity assays were carried out by a discontinuous assay with cells suspended in M9-G in a final volume of 500 μl at 25°C. For determination of the kinetic parameters for the conversion of benzene to phenol, cells were used at an optical density corresponding to 0.5 mU/ml for cells expressing ToMO and 1 mU/ml for cells expressing the PH complex. Reactions were started by the addition of various amounts of benzene in *N*,*N*-dimethylformamide to cell suspensions and stopped at different times by the addition of 50 μl of 1 M HCl. Samples were centrifuged at 12,000 rpm for 20 min at 4°C. Soluble fractions were stored at −20°C until analysis. Phenol and catechol, the products of benzene oxidation, were separated by HPLC on an Ultrasphere C_{18} reverse-phase column (4.6 by 250 mm, 80-Å pore size), monitoring the absorbance of the eluate at 274 nm. Separation was carried out at a flow rate of 1 ml/min with a linear gradient of a two-solvent system made up of water containing 0.1% formic acid (solvent A) and methanol containing 0.1% formic acid (solvent B). Phenol and catechol were separated by a 12-min isocratic elution at 10% solvent B, followed by a linear gradient ranging from 10 to 30% solvent B over 10 min and an isocratic step at 30% solvent B. The amount of each product was determined by comparing the area of each peak with that obtained by the same chromatography procedure on standard solutions.

Time course of benzene oxidation. The rate of formation of products from benzene catalyzed by *E. coli* cells expressing PH or ToMO or a mixture of both types of cells was measured (i) by the discontinuous assay for monitoring the rate of formation of phenol and catechol or (ii) by the continuous assay for monitoring only the rate of formation of catechol. When the discontinuous assay was used, cells were used at an optical density corresponding to 1 mU/ml, with 30 μM benzene.

When the continuous assay was used, cells were incubated in a closed quartz cuvette in a final volume of 500 μl of M9-G, 3 U of C2,3O, and 30 μM benzene. Cells were suspended at the appropriate concentration, as described in the Results section.

Kinetic parameter determination. Kinetic parameters were calculated with the program GraphPad Prism (GraphPad Software). For the assays carried out with cells, the protein concentration was determined by densitometric scanning of SDS-PAGE assays of cell extracts.

Other methods. Homology studies were performed by searching the public nucleotide and protein databases with BLAST. ClustalW was used to obtain multiple alignments for each subunit. Identification of the cofactor flavin adenine dinucleotide (FAD) from PH P was performed as already described (24). Iron, labile sulfide, and FAD contents were determined as already described (6). SDS-PAGE analysis, N-terminal protein sequence determinations, electrospray mass spectrometric measurements, MALDI/mass spectrometry (MALDI/MS) analysis of peptide mixtures, and determination of the molecular weights by gel filtration were performed as already described (31). Subunits L, N, and O from the PH (LNO) subcomplex were separated by HPLC with a Phenomenex Jupiter narrow-bore C_4 column (2.1 by 250 mm, 300-Å pore size), at a flow rate of 0.2 ml/min with a linear gradient of a two-solvent system. Solvent A was 0.1% trifluoroacetic acid in water, and solvent B was acetonitrile containing 0.07% trifluoroacetic acid. Proteins were separated by a linear gradient ranging from 10 to 65% solvent B over 60 min. In the case of the liquid chromatography (LC)/MS analysis of subunits PH P and PH M, the same column was used with a linear gradient ranging from 10 to 95% solvent B over 20 min.

Nucleotide sequence accession number. The nucleotide sequence of the *ph* locus was submitted to GenBank and given accession number AY205602.

RESULTS

Nucleotide sequence of the phenol hydroxylase locus. The locus coding for phenol hydroxylase (*ph*) has already been mapped on a 4.8-kb SacI-XbaI fragment of the *P. stutzeri* OX1 chromosome cloned in pJSX148 (1). The nucleotide sequence of the *ph* locus was determined as described in Materials and Methods. Translation of the sequence in all possible reading frames revealed the presence of five open reading frames, named *ph l, m, n, o*, and *p*.

Comparison of the five predicted polypeptide sequences with the nonredundant peptide sequence database at the European Biology Institute revealed homology with the subunits of several multicomponent phenol hydroxylases and T2MOs, most notably with the phenol hydroxylase from *Pseudomonas* sp. strain CF600 (20). The degree of identity of subunits L, M, N, O, and P with the homologous subunits from *Pseudomonas* sp. strain CF600 PH was found to be 63, 68, 76, 53, and 77%, respectively, whereas the degree of identity with the homologous subunits of T2MO from *B. cepacia* G4 (19) was significantly lower, 43, 43, 62, 39, and 56%, respectively. It is noteworthy that the three enzymes have the same number and type of subunits, and the corresponding open reading frames were found in the same order in the operons. It should also be noted that the degree of identity of *P. stutzeri* PH with other toluene monooxygenases such as ToMO and T4MO was found to be lower. In fact, only subunits L, M, N, and P of PH found counterparts in subunits E, D, A, and F of ToMO, respectively, with identities of 20, 27, 21, and 24%, respectively.

As *Pseudomonas* sp. strain CF600 PH and T2MO from *B. cepacia* G4 belong to the group 1 BMMs (21), it may be concluded that the phenol hydroxylase from *P. stutzeri* OX1 is a multicomponent enzyme belonging to the same group.

Characterization of the recombinant subunits of the PH complex. (i) PH (LNO) subcomplex. Subunits PH O, L, and N, expressed from the *ph* cluster cloned into vector pJSX148 and purified, coeluted in a single peak in all the chromatographic systems used (data not shown).

When the sample containing the three proteins derived from the final gel filtration step of the purification procedure was subjected to molecular weight determination by gel filtration on Superose 12 PC 3.2/30, a single peak was obtained, with an apparent molecular mass of 220 kDa.

Samples of the purified LNO subcomplex were also analyzed by LC/MS after their separation by HPLC. Components O, L, and N showed molecular masses of 13,103.4 ± 0.2, 38,280.4 ± 1.9, and 60,010 ± 4 Da, respectively. These values are in agreement with the expected molecular masses calculated on the basis of the deduced amino acid sequence of the mature forms of the subunits, as reported in GenBank at accession number AY205602.

The primary structure of each of the recombinant subunits of the LNO subcomplex was verified by peptide mapping, as reported in Materials and Methods. The results led to complete verification of the amino acid sequences of subunits O, L, and N. Finally, the iron content of the complex was determined and found to be 1.44 mol/mol of (LNO).

(ii) PH P and PH M. Attempts to purify adequate amounts of subunits PH P and PH M from the expression of the entire *ph* cluster in pJSX148 were unsuccessful. We thus subcloned the sequences coding for the two subunits into the expression vector pET22b(+), equipped with a strong ribosome-binding site located 9 bp upstream of the start codon. This strategy proved to be fruitful, as we were able to purify about 14 and 3 mg of pure PH P and PH M, respectively, per liter of culture.

Samples of purified PH P were analyzed by LC/MS. The recombinant protein showed a molecular mass of 38,439.4 ± 1.5 Da. This value is in agreement with the expected molecular mass calculated on the basis of the deduced amino acid sequence of the mature form of the subunit, as reported in GenBank at accession number AY205602. The primary structure of recombinant PH P was verified by peptide mapping, and the results led to complete verification of the amino acid sequence.

The spectrum of purified PH P showed typical maxima at 273, 340, 392, and 460 nm, like other reductase components of various bacterial oxygenases (24, 27), and consistent with the presence of a [2Fe-2S] iron-sulfur cluster and a flavin cofactor. The cofactor was identified to be FAD by thin-layer chromatography experiments. Moreover, the amount of bound FAD was calculated to be 0.8 to 0.9 mol/mol of protein, which indicates that 1 mol of PH P binds 1 mol of FAD. The presence of iron and sulfur was verified by colorimetric analyses. The molar ratio of iron to protein was found to be 2 ± 0.1, whereas the sulfide content was 2.7 ± 0.3 mol/mol of protein. These results are in agreement with a presence of a [2Fe-2S] cluster. Moreover, a molar extinction coefficient at 460 nm was calculated on several preparations and found to be 21,000 M^{-1} cm^{-1}.

PH P was found to reduce several artificial electron acceptors such as horse heart cytochrome *c*, 2,6-dichlorophenolindophenol, and potassium ferricyanide, with either NADH or NADPH as the electron donor. The specific activity on cytochrome *c* calculated on several purifications was 178.13 ± 11.02 U per mg of purified PH P. NADH and NADPH oxidation was found to follow Michaelis-Menten kinetics, with an apparent K_m of 37.79 μM for NADH and 900 μM for NADPH. Hence, the replacement of NADPH for NADH produces a 23.8-fold increase in the K_m, which indicates that PH P preferentially uses NADH as an electron donor.

Samples of purified PH M were analyzed by LC/MS. The recombinant protein showed a molecular mass of 10,347.9 ± 0.46. This value is in good agreement with that expected on the basis of the deduced amino acid sequence of the mature form of the subunit, as reported in GenBank at accession number AY205602. Also, the primary structure of PH M was verified by the peptide-mapping strategy. The results led to complete verification of its amino acid sequence.

Single-turnover assays. To positively identify the hydroxylase component of the complex, we performed single-turnover assays by measuring the ability of PH (LNO), PH P, and PH M, and their combinations to oxidize phenol to catechol. The results of the experiments, with sodium dithionite as a reductant and methyl viologen as a redox mediator, are reported in Table 1. They indicate that PH (LNO) alone, in the absence of any other protein expressed by the *ph* cluster, is able to convert phenol into catechol, whereas PH P alone and PH M alone are not able to convert phenol into catechol.

The data reported in Table 1 also show that the addition of PH P to PH (LNO) increases the amount of the product

TABLE 1. Single-turnover assays catalyzed by the components of the phenol hydroxylase complex[a]

Component(s)	Catechol produced (nmol)	Yield (%)
PH (LNO)	0.132	1.2
PH P	0	
PH M	0	
PH (LNO) + PH M	0.169	1.5
PH (LNO) + PH P	0.328	3.1
PH (LNO) + PH M + PH P	1.58	14.7

[a] The experiments were performed as described in Materials and Methods with 10.7 nmol of PH (LNO), 14 nmol of PH M, and 12.25 nmol of PH P. PH P and PH (LNO) were added in the oxidized form and reduced by the addition of dithionite. The amounts of catechol produced are averages (± 10%) of values obtained by various determinations carried out with different preparations of the subunits. Yield was calculated as the ratio of the amount of catechol produced with respect to the amount of the hydroxylase component in the assay.

2.48-fold, whereas the addition of PH M to PH (LNO) is almost ineffective. On the other hand, when all three components, PH M, PH P, and PH (LNO) are present, a 12-fold increase in the amount of product with respect to that produced in the presence of PH (LNO) alone is observed.

In vitro reconstitution of the PH complex. Preliminary multiple-turnover activity assays indicated that mixtures of equimolar amounts of the purified PH components, PH (LNO), PH P, and PH M, were able to transform phenol into catechol.

To determine the optimal relative concentration of each subunit for obtaining maximum hydroxylase activity, we carried out kinetic measurements with mixtures of PH (LNO), P, and M in which the concentration of each single component was changed with respect to the other components.

Figure 2 shows the effects on the rate of reaction of increasing ratios of PH M (Fig. 2A) and PH P (Fig. 2B) with respect to PH (LNO) in the presence of constant amounts of the other components.

Figure 2A shows that a linear relationship is obtained at low ratios of PH M, followed by a sharp break at about 0.8 mol of PH M/mol of PH (LNO). Ratios of PH M/mol of PH (LNO) higher than 2 inhibited the phenol hydroxylase activity.

PH P showed instead a different behavior (Fig. 2B), as no titration break was detectable, and the rate of reaction increased with the concentration of PH P, although the increase was less pronounced at high concentration of the reductase component and saturation was reached at molar ratios higher than 6.

Based on the titration experiments described above, we measured the kinetic parameters of the reconstituted complex, with the ratios LNO:M:P = 1:1.4:6. The specific activity was 185.55 ± 12.26 nmol of phenol converted per min per mg of (LNO), whereas k_{cat} and K_m values were 0.286 ± 0.009 s^{-1} and 0.61 ± 0.09 μM, respectively.

Moreover, we also measured the rates of phenol hydroxylation and NADH oxidation at different PH P concentrations in the presence of fixed amounts of PH (LNO) and PH M (data not shown). We found a stoichiometric ratio between the amount of NADH oxidized and the amount of catechol produced up to a molar ratio of PH P to PH (LNO) of less than 0.5. At higher PH P:PH (LNO) ratios, the rate of NADH oxidation is higher than that of catechol formation.

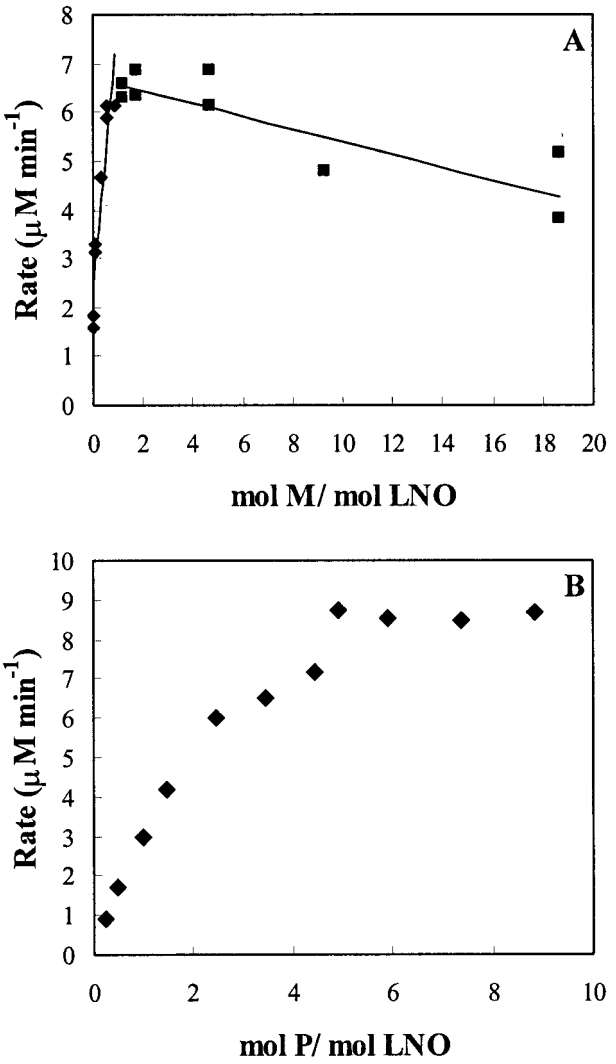

FIG. 2. Effect of different concentrations of PH P (A) and PH M (B) with respect to the hydroxylase component on the rate of catechol production. Activity was measured as described in Materials and Methods. Curve A represents PH LNO at 0.288 μM and PH P at 0.990 μM. Curve B represents PH LNO at 0.288 μM and PH M at 0.503 μM.

Substrate specificity of ToMO and PH complexes. We investigated the substrate specificity of ToMO and PH complexes by measuring the kinetic parameters of the two enzymes on benzene and phenol as substrates, with *E. coli* cells expressing the PH or ToMO complex. The assays were carried out as described in Materials and Methods and yielded the kinetic parameters reported in Table 2.

The time course of phenol and catechol production by *E. coli* cells expressing ToMO or PH was determined by their incubation with 30 μM benzene in the discontinuous assay described in Materials and Methods, at an optical density corresponding to 1 mU/ml.

As shown in Fig. 3A, when cells expressing ToMO were used, phenol was produced at a linear rate of about 0.4 μM min^{-1}, whereas catechol was not detected up to 35 to 40 min, and its formation started after about 60 min.

On the other hand, when cells expressing PH were used, the

TABLE 2. Kinetic constants of PH and ToMO on benzene and phenol[a]

Substrate	PH			ToMO		
	k_{cat} (s^{-1})	K_m (μM)	k_{cat}/K_m (10^3 s^{-1} μM^{-1})	k_{cat} (s^{-1})	K_m (μM)	k_{cat}/K_m (10^3 s^{-1} μM^{-1})
Benzene (cells)	0.092	25	3.7	0.36	~0.2	1,810
Phenol (cells)	1.02	0.6	1,696	1.00	2.18	460
Phenol (complex)	0.286	0.61	469			

[a] Constants were measured on cells (benzene and phenol) or on the reconstituted complex (phenol). Errors were always lower than 6% except those for K_m on benzene, which was about 25%.

phenol concentration reached a constant but low value after 25 to 30 min, whereas catechol could be detected even at short times, and its concentration increased with time (Fig. 3B).

A different picture emerged when the same experiment was carried out by monitoring only catechol formation for 15 min by the C2,3O-coupled continuous assay.

The data tabulated in Fig. 4 indicate that, as shown in the experiment monitored by the discontinuous assay, neither cells expressing ToMO (tested at three different optical densities corresponding to 0.27, 0.55, and 1.1 mU/ml) nor cells expressing PH (0.22 mU/ml) efficiently produced catechol, although a small amount was formed in the latter case, at a rate of 0.017 μM min^{-1}.

Surprisingly, instead, a mixture of the two types of cells efficiently produced catechol. When cells expressing PH at an optical density corresponding to 0.22 mU/ml were mixed with ToMO-expressing cells at 0.27 mU/ml, the rate of formation of catechol was nine times higher than that measured when the cells were used separately. Moreover, when increasing amounts of cells expressing ToMO (0.55 and 1.1 mU/ml) were mixed with a constant amount of cells expressing PH (0.22 mU/ml), the rate of formation of catechol was found to be 13 and 19 times higher, respectively, than that observed with PH-expressing cells alone.

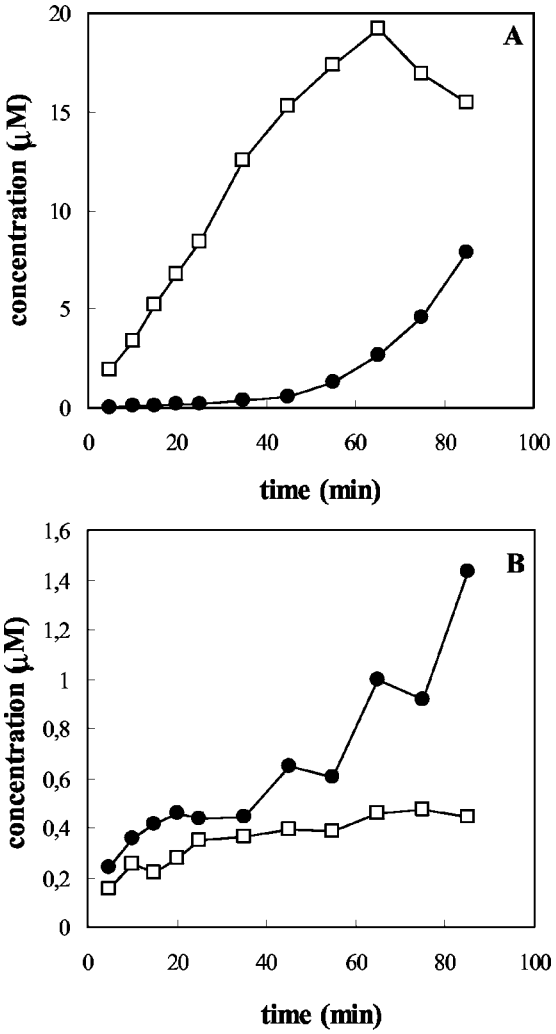

FIG. 3. Kinetics of phenol (open squares) and catechol (solid circles) production by (A) cells expressing ToMO at 1 mU/ml and (B) PH at 1 mU/ml, incubated with 30 μM benzene.

DISCUSSION

Characterization of the PH complex. The homology studies of the *P. stutzeri* OX1 PH subunits have shown that PH is a multicomponent protein belonging to group 1 BMMs that includes well-characterized enzymes such as PH from *Pseudo-*

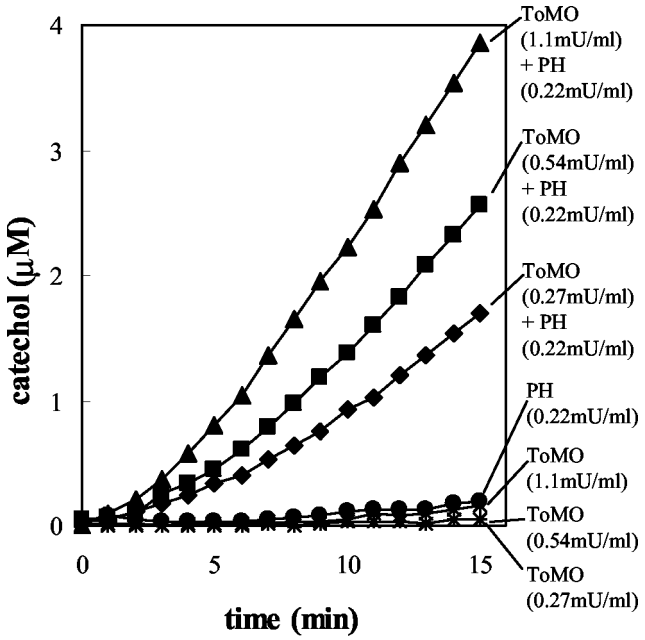

FIG. 4. Kinetics of catechol production by cells expressing ToMO or PH incubated with 30 μM benzene. Catechol was measured by the C2,3O-coupled colorimetric assay described in Materials and Methods.

monas sp. strain CF600 and T2MO from *B. cepacia* G4 (19, 20) and is more closely related to the *Pseudomonas* sp. strain CF600 enzyme. Subunits L, N, and O find their counterparts in polypeptides that are part of the hydroxylase components of monooxygenase systems (15, 19, 28, 34, 36). It is noteworthy that the general structure of these hydroxylase complexes is dimeric, and each single monomeric unit is made up of two or three protomers. The findings that subunits L, N, and O coelute in a single peak in all chromatographic systems used and that the apparent molecular mass of the complex is 220 kDa strongly support the hypothesis that subunits L, N, and O of *P. stutzeri* OX1 PH also constitute a dimeric $(LNO)_2$ subcomplex (whose expected molecular mass is 222,786 Da). Moreover, its iron content is about 1.5 mol/mol of (LNO). This result is in agreement with the presence of a diiron center in each of the N subunits, as suggested by its homology with other monooxygenase "large" subunits (25, 28, 38).

Finally, single-turnover assays have shown that PH $(LNO)_2$ alone, in the absence of any other PH component, is able to convert phenol into catechol, confirming its identification with the hydroxylase component of the complex, in agreement with homology studies (1).

As for PH P, homology studies have shown that this subunit is homologous to the reductase components of other BMMs. The spectrum of purified PH P is consistent with the presence of a [2Fe-2S] iron-sulfur cluster and a flavin cofactor, and 1 mol of FAD and a single [2Fe-2S] cluster are found per mol of PH P. Moreover, PH P can reduce several artificial electron acceptors with either NADH or, less efficiently, NADPH as the electron donor. Thus, all of the data lead to the identification of subunit PH P with the NAD(P)H-oxidoreductase component of the PH complex. PH P is not able to convert phenol into catechol in single-turnover experiments, but its addition to the hydroxylase subcomplex $(LNO)_2$ increased the amount of the product produced 2.48-fold (Table 1). This increase may well be attributed to the ability of artificially reduced PH P to transfer additional electrons to PH (LNO), thus promoting more than one reaction cycle in the single-turnover assay.

As for PH M, homology studies have indicated that it is homologous to the small regulatory proteins of BMMs. These proteins are required for catalysis (14) but contain neither organic cofactor nor metal ions, and it is unlikely that they participate directly in the electron transfer (14). Thus, given the identification of PH P with the NADH-oxidoreductase component of the PH complex, it may be hypothesized that PH M is the effector protein of the complex. PH M alone is not able to convert phenol into catechol in single-turnover experiments, and unlike PH P, its addition to the hydroxylase subcomplex $(LNO)_2$ was almost ineffective. On the other hand, when PH M was added to mixtures of PH P and PH $(LNO)_2$, the amount of the product increased 4.8-fold with respect to that produced in the presence of PH $(LNO)_2$ plus PH P and 12-fold with respect to that produced in the presence of the hydroxylase subcomplex alone. This may indicate that cooperative interactions between the three components occur, suggestive of the formation of a ternary complex, as has been demonstrated for other homologous monooxygenases (9, 10), and that PH M may enhance coupling in the system, as has been recently reported for methane monooxygenase B (MMO B) from *Methylosinus trichosporium* OB3b (35).

Finally, the yield of product formation by the reconstituted complex measured in single-turnover assays (Table 1), although low, is similar to yields determined for other monooxygenase complexes (5, 19, 25). This might be an indication of uncoupling and/or of the presence of inactive protein species.

In vitro reconstitution of the PH complex. To test the ability of the individually purified components PH $(LNO)_2$, PH P, and PH M to reconstitute a functional complex, we carried out in vitro experiments to measure the ability of mixtures of the components to catalyze the conversion of a substrate into a product mediated by electrons coming from the donor.

Increasing ratios of PH M with respect to PH (LNO) in the presence of constant amounts of PH P increased the rate of product formation (Fig. 2A), until a sharp break was observed. The nearly linear titration and the break are indications of a high affinity of this component for the LNO subcomplex, as already observed for the regulatory component of methane monooxygenase (9). At higher concentrations, PH M inhibited the reaction (Fig. 2A), as reported for other regulatory components (9). This might be due to a reduction in coupling efficiency, as recently demonstrated for T4MO (18).

On the contrary, no titration break was present when PH M was held constant and PH P was increased (Fig. 2B). This result suggests that the association of PH P in the complex is weaker than that of PH M. It should also be noted that the ratio of moles of PH P to moles of PH (LNO) at which we observed the maximum velocity is similar to the values determined for the homologous phenol hydroxylase from *Pseudomonas* sp. strain CF600 (5) and for the phenol hydroxylase from *Acinetobacter radioresistens* S13 (12).

Moreover, we have observed that NADH is consumed at a stoichiometric ratio with respect to catechol produced, with PH P:PH (LNO) ratios lower than 0.5. This indicates that, at least under these conditions, NADH oxidation is completely coupled to substrate oxidation. The fact that at PH P:PH (LNO) ratios higher than 0.5 the rate of NADH oxidation is higher than that of catechol formation could indicate some uncoupling, as already observed in other monooxygenase systems (10, 11, 18, 23).

As for the kinetic parameters determined for the reconstituted complex (Table 2), it should be noted that the K_m of the PH from *P. stutzeri* for benzene is similar to that reported for T4MO for the same substrate (26). In contrast, the k_{cat} value of PH on benzene is one order of magnitude lower than that reported for T4MO (26) and four times lower than that of ToMO (Table 2). This might be an indication that ToMO and T4MO are better catalysts for the transformation of nonhydroxylated substrates than PH. This hypothesis is reinforced by the observation that the k_{cat} values on phenol of two different phenol hydroxylases, one from *P. stutzeri* and one from *Acinetobacter radioresistens* (8), are of the same order of magnitude.

Finally, the kinetic parameters determined for the reconstituted complex with saturating ratios of each component are similar to those measured with *E. coli* cells expressing the entire PH complex from vector pJSX148 (Table 2). This leads us to conclude that the purified recombinant components are able to reconstitute an active PH complex in which all individual subunits are functional.

Metabolic roles of ToMO and PH. Genes for ToMO and PH are both present in the genome of *P. stutzeri* OX1. The exper-

iments described in this paper indicate that the expression of the gene cluster coding for PH leads to a functional complex, as has already been demonstrated in the case of the ToMO complex (6).

It has already been shown that ToMO is able to oxidize a variety of aromatic substrates, including *o*-, *m*-, and *p*-cresol, phenol, toluene, benzene, and naphthalene (3). PH is also able to oxidize phenol and *o*-, *m*-, and *p*-cresol (1). Moreover, as shown in Table 2, it oxidizes benzene as well. Thus, it would appear that two apparently similar functions, i.e., two enzymes involved in the catalysis of identical or similar reactions, are present in the same microorganism.

To shed light on the apparent redundancy of hydroxylase functions in the same microorganism, we investigated the kinetics and the substrate specificity of both complexes by measuring the kinetic parameters of the two enzymes on benzene and phenol with *E. coli* cells expressing PH and ToMO complexes from vectors pJSX148 and pBZ1260, respectively.

Both ToMO and PH (E, enzyme) catalyze the conversion of benzene (B) into catechol (C) in a two-step process, involving phenol (P) as an intermediate, according to the equation

$$E + B \underset{}{\overset{K_m^B}{\rightleftharpoons}} EB \xrightarrow{k_{cat}^B} E + P \underset{}{\overset{K_m^P}{\rightleftharpoons}} EP \xrightarrow{k_{cat}^P} E + C \quad (1)$$

where k_{cat}^B and k_{cat}^P are the catalytic constants for benzene and phenol, respectively, and K_m^B and K_m^P are the Michaelis constants for the two reactions.

However, the kinetic characterization of the two enzymes, although restricted to few substrates, would indicate that their behavior is quite different. ToMO shows a specificity constant in the first step which is about fourfold higher than in the second step (Table 2). On the other hand, the catalytic parameters of PH on the same substrates allow us to draw a different picture. In contrast to the values determined for ToMO, the k_{cat}/K_m of PH for phenol is about 460-fold higher than that for benzene (Table 2). This difference depends on both the K_m and k_{cat} values. In fact, the K_m for benzene is about 40-fold higher than that for phenol, whereas its k_{cat} value for phenol is almost 10-fold higher than that for benzene.

These data lead to the conclusion that PH hydroxylates phenol much more efficiently than benzene, which, in turn, is preferentially transformed by ToMO, as indicated by its high specificity constant for this substrate compared with that of PH.

What can be the reason for the presence of these two enzymes in the same microorganism? It should be remembered that both enzymes are part of the upper pathway, which is responsible for the degradation of aromatic hydrocarbons. It can be reasonably hypothesized that both enzymes serve the purpose of effectively channeling aromatic substrates to the lower pathway, which is initiated by C2,3O. Thus, the metabolic importance of the two enzymes can be evaluated on the basis of their ability to produce catechol, i.e., the substrate of C2,3O.

To this purpose, we experimentally determined the amounts of phenol and catechol which are produced from benzene as a function of time (Fig. 3A and B). When *E. coli* cells expressing ToMO were incubated with 30 μM benzene (a concentration 100-fold higher than the K_m), phenol was produced at a linear rate, whereas catechol could not be detected for 35 to 40 min, and it began to be produced only after about 60 to 70% of the benzene had been converted to phenol (Fig. 3A). This behavior is consistent with the sequential action of the enzyme on benzene and phenol, as described by equation 1, and with its kinetic parameters (Table 2).

According to the Michaelis-Menten model, the rates of the two steps in equation 1 are:

$$v_1 = (k_{cat}^B/K_m^B)\,[E]\,[B] \quad (2)$$

$$v_2 = (k_{cat}^P/K_m^P)\,[E]\,[P] \quad (3)$$

Hence, the ratio v_1/v_2, which gives a measure of the relative efficiency of the enzyme in the two steps, is given by

$$v_1/v_2 = k_{cat}^B K_m^P\,[B]/k_{cat}^P K_m^B\,[P] \quad (4)$$

Substituting the experimentally determined catalytic constants, equation 4 gives $v_1/v_2 = 3.93$ [B]/[P]. Therefore when [B] = 10 [P], then $v_1/v_2 = 39.3$. Thus, under these conditions, the first step of the reaction is about 40-fold faster than the second. When [B] = [P], then $v_1/v_2 = 3.93$, and only when [P] = 3.93 [B] does $v_1 = v_2$. Thus, the simple application of the Michaelis-Menten model to the conversion of benzene into catechol catalyzed by ToMO indicates that a saturating benzene concentration acts as an inhibitor of the second hydroxylation step and that catechol is not produced until the phenol concentration is higher than the benzene concentration. This result is in perfect agreement with the experimentally determined data.

When *E. coli* cells expressing PH were incubated with 30 μM benzene, in contrast to what was observed in the case of ToMO, no lag in the production of catechol was observed. However, this is not a very efficient process because the reaction is limited by the amount of phenol produced in the first step, which soon reaches a low and constant value (Fig. 3B). When equation 4 is solved with the kinetic constants experimentally determined for PH, the ratio v_1/v_2 is 0.0022 [B]/[P]. Hence, even when [B] = 10[P], the second step is 45-fold faster than the first, and it becomes 450-fold faster when [B] = [P]. Therefore, equation 4 allows us to predict that when benzene is used as a substrate by PH, it is slowly converted to phenol, which in turn is very efficiently oxidized to catechol. This conclusion is in line with the experimentally observed behavior.

Finally, comparison of the specificity constants of ToMO and PH on benzene shows that the k_{cat}/K_m of ToMO is about 500-fold higher than that of PH, whereas the specificity constant of PH on phenol is only 4-fold higher than that of ToMO. Thus, we can predict that when both enzymes compete for benzene as a substrate, ToMO will efficiently produce phenol, which in turn will be very efficiently oxidized to catechol by PH. The results obtained by observing benzene oxidation by a mixture of cells expressing ToMO and PH support this hypothesis. In fact, as shown in Fig. 4, ToMO alone did not form any significant amount of catechol from benzene, whereas only small amounts were produced by PH alone. When mixtures of both types of cells were used, catechol was produced at a rate that was proportional to the concentration of ToMO-expressing cells and more than one order of magnitude higher than that measured with PH alone.

Thus, we can confidently conclude that the concerted use of

ToMO and PH optimizes the use of benzene in *P. stutzeri* OX1 by the draining effect of PH on the products of oxidation catalyzed by ToMO, which in turn excludes the possibility that phenols will accumulate.

ACKNOWLEDGMENTS

We are indebted to Giuseppe D'Alessio, Department of Biological Chemistry, University of Naples Federico II, for critically reading the manuscript. We also thank P. Barbieri (Dipartimento di Biologia Strutturale e Funzionale, Università dell'Insubria, Varese, Italy) for kindly providing the cDNA coding for the *ph* cluster.

This work was supported by grants from the Ministry of University and Research (PRIN/2000 and PRIN/2002).

REFERENCES

1. **Arenghi, F. L., D. Berlanda, E. Galli, G. Sello, and P. Barbieri.** 2001. Organization and regulation of meta cleavage pathway gene for toluene and *o*-xylene derivative degradation in *Pseudomonas stutzeri* OX1. Appl. Environ. Microbiol. **67:**3304–3308.
2. **Baggi, G., P. Barbieri, E. Galli, and S. Tollari.** 1987. Isolation of a *Pseudomonas stutzeri* strain that degrades *o*-xylene. Appl. Environ. Microbiol. **53:** 2129–2131.
3. **Bertoni, G., F. Bolognesi, E. Galli, and P. Barbieri.** 1996. Cloning of the genes for and characterization of the early stages of toluene catabolism in *Pseudomonas stutzeri* OX1. Appl. Environ. Microbiol. **62:**3704–3711.
4. **Bertoni, G., M. Martino, E. Galli, and P. Barbieri.** 1998. Analysis of the gene cluster encoding toluene/*o*-xylene monooxygenase from *Pseudomonas stutzeri* OX1. Appl. Environ. Microbiol. **64:**3626–3632.
5. **Cadieux, E., V. Vrajmasu, C. Achim, J. Powlowski, and E. Munck.** 2002. Biochemical, Mossbauer, and EPR studies of the diiron cluster of phenol hydroxylase from Pseudomonas sp. strain CF 600. Biochemistry **41:**10680–10691.
6. **Cafaro, V., R. Scognamiglio, A. Viggiani, V. Izzo, I. Passaro, E. Notomista, F. Dal Piaz, A. Amoresano, A. Casbarra, P. Pucci, and A. Di Donato.** 2002. Expression and purification of the recombinant subunits of toluene/o-xylene monooxygenase and reconstitution of the active complex. Eur. J. Biochem. **269:**5689–5699.
7. **Chauhan, S., P. Barbieri, and T. Wood.** 1998. Oxidation of trichloroethylene, 1,1-dichloroethylene, and chloroform by toluene/*o*-xylene monooxygenase from *Pseudomonas stutzeri* OX1. Appl. Environ. Microbiol. **64:**3023–3024.
8. **Divari, S., F. Valetti, P. Caposio, E. Pessione, M. Cavaletto, E. Griva, G. Gribaudo, G. Gilardi, and C. Giunta.** 2003. The oxygenase component of phenol hydroxylase from Acinetobacter radioresistens S13. Eur. J. Biochem. **270:**2244–2253.
9. **Fox, B. G., Y. Liu, J. E. Dege, and J. D. Lipscomb.** 1991. Complex formation between the protein components of methane monooxygenase from *Methylosinus trichosporium* OB3b. Identification of sites of component interaction. J. Biol. Chem. **266:**540–550.
10. **Fox, G. B., W. A. Froland, J. E. Dege, and J. D. Lipscomb.** 1989. Methane monooxygenase from *Methylosinus trichosporium* OB3b. J. Biol. Chem. **264:** 10023–10033.
11. **Green, J., and H. Dalton.** 1985. Protein B of soluble methane monooxygenase from *Methylococcus capsulatus* (Bath). A novel regulatory protein of enzyme activity. J. Biol. Chem. **260:**15795–15801.
12. **Griva E., P. E., Divari S., Valletti F., Cavaletto M., Rossi GL., Giunta C.** 2003. Phenol hydroxylase from Acinetobacter radioresistens S13. Eur. J. Biochem **270:**1434–1440.
13. **Harayama, S., and M. Rekik.** 1989. Bacterial aromatic ring-cleavage enzymes are classified into two different gene families. J. Biol. Chem. **264:** 15328–15333.
14. **Hemmi, H., J. M. Studts, Y. K. Chae, J. Song, J. L. Markley, and B. G. Fox.** 2001. Solution structure of the toluene 4-monooxygenase effector protein (T4moD). Biochemistry **40:**3512–3524.
15. **Johnson, G. R., and R. H. Olsen.** 1995. Nucleotide sequence analysis of genes encoding a toluene/benzene-2-monooxugenase from *Pseudomonas* sp. strain JS150. Appl. Environ. Microbiol. **61:**3336–3346.
16. **Kahng, H. Y., J. C. Malinverni, M. M. Majko, and J. J. Kukor.** 2001. Genetic and functional analysis of the *tbc* operons for catabolism of alkyl- and chloroaromatic compounds in *Burkholderia* sp. strain JS150. Appl. Environ. Microbiol. **67:**4805–4816.
17. **Matsudaira, P.** 1987. Sequence from picomole quantities of proteins electroblotted onto polyvinylidene difluoride membranes. J. Biol. Chem. **262:** 10035–10038.
18. **Mitchell, K. H., J. M. Studts, and B. G. Fox.** 2002. Combined participation of hydroxylase active site residues and effector protein binding in a para to ortho modulation of toluene 4-monooxygenase regiospecificity. Biochemistry **41:**3176–3188.
19. **Newman, L. M., and L. P. Wackett.** 1995. Purification and characterization of toluene 2-monooxygenase from *Burkholderia cepacia* G4. Biochemistry **34:** 14066–14076.
20. **Nordlund, I., J. Powlowski, and V. Shingler.** 1990. Complete nucleotide sequence and polypeptide analysis of multicomponent phenol hydroxylase from *Pseudomonas* sp. strain CF600. J. Bacteriol. **172:**6826–6833.
21. **Notomista, E., A. Lahm, A. Di Donato, and A. Tramontano.** 2003. Evolution of bacterial and archaeal multicomponent monooxygenases. J. Mol. Evol. **56:**435–445.
22. **Olsen, R. H., J. J. Kukor, and B. Kaphammer.** 1994. A novel toluene-3-monooxygenase pathway cloned from *Pseudomonas pickettii* PKO1. J. Bacteriol. **176:**3748–3756.
23. **Oppenheim, S. F., J. M. Studts, B. G. Fox, and J. S. Dordick.** 2001. Aromatic hydroxylation catalyzed by toluene 4-monooxygenase in organic solvent/aqueous buffer mixtures. Appl. Biochem. Biotechnol. **90:**187–197.
24. **Pessione, E., S. Divari, E. Griva, M. Cavaletto, G. L. Rossi, G. Gilardi, and C. Giunta.** 1999. Phenol hydroxylase from *Acinetobacter radioresistens* is a multicomponent enzyme. Eur. J. Biochem. **265:**549–555.
25. **Pikus, J. D., J. M. Studts, C. Achim, K. E. Kauffmann, E. Munck, R. J. Steffan, K. McClay, and B. G. Fox.** 1996. Recombinant toluene-4-monooxygenase: catalytic and Mossbauer studies of the purified diiron and rieske components of a four-protein complex. Biochemistry **35:**9106–9119.
26. **Pikus, J. D., J. M. Studts, K. McClay, R. J. Steffan, and B. G. Fox.** 1997. Changes in the regiospecificity of aromatic hydroxylation produced by active site engineering in the diiron toluene 4-monooxygenase. Biochemistry **36:** 9283–9289.
27. **Powlowski, J., and V. Shingler.** 1990. In vitro analysis of polypeptide requirements of multicomponent phenol hydroxylase from *Pseudomonas* sp. strain CF600. J. Bacteriol. **172:**6834–6840.
28. **Rosenzweig, A. C., C. A. Frederick, S. J. Lippard, and P. Nordlund.** 1993. Crystal structure of a bacterial non-heme iron hydroxylase that catalyses the biological oxidation of methane. Nature **366:**537–543.
29. **Ryoo, D., H. Shim, K. Canada, P. Barbieri, and T. K. Wood.** 2000. Aerobic degradation of tetrachloroethylene by toluene-o-xylene monooxygenase of *Pseudomonas stutzeri* OX1. Nat. Biotechnol. **18:**775–778.
30. **Sambrook, J., E. F. Fritsch, and T. Maniatis.** 1989. Molecular cloning: a laboratory manual, 2nd ed. Cold Spring Harbor Laboratory Press, Cold Spring Harbor, N.Y.
31. **Scognamiglio, R., E. Notomista, P. Barbieri, P. Pucci, F. Dal Piaz, A. Tramontano, and A. Di Donato.** 2001. Conformational analysis of putative regulatory subunit D of the toluene/o-xylene-monooxygenase complex from *Pseudomonas stutzeri* OX1. Protein Sci. **10:**482–490.
32. **Shaw, J. P., and S. Harayama.** 1992. Purification and characterisation of the NADH:acceptor reductase component of xylene monooxygenase encoded by the TOL plasmid pWW0 of *Pseudomonas putida* mt-2. Eur. J. Biochem. **209:**51–61.
33. **Shields, M. S., S. O. Montgomery, P. J. Chapman, S. M. Cuskey, and P. H. Pritchard.** 1989. Novel pathway of toluene catabolism in the trichloroethylene-degrading bacterium G4. Appl. Environ. Microbiol. **55:**1624–1629.
34. **Small, F. J., and S. A. Ensign.** 1997. Alkene monooxygenase from *Xanthobacter strain* Py2. Purification and characterization of a four-component system central to the bacterial metabolism of aliphatic alkenes. J. Biol. Chem. **272:**24913–24920.
35. **Wallar, B. J., and J. D. Lipscomb.** 2001. Methane monooxygenase component b mutants alter the kinetics of steps throughout the catalytic cycle. Biochemistry **40:**2220–2233.
36. **Whited, G. M., and D. T. Gibson.** 1991. Toluene-4-monooxygenase, a three-component enzyme system that catalyzes the oxidation of toluene to *p*-cresol in *Pseudomonas mendocina* KR1. J. Bacteriol. **173:**3010–3016.
37. **Yen, K. M., M. R. Karl, L. M. Blatt, M. J. Simon, R. B. Winter, P. R. Fausset, H. S. Lu, A. A. Harcourt, and K. K. Chen.** 1991. Cloning and characterization of a *Pseudomonas mendocina* KR1 gene cluster encoding toluene-4-monooxygenase. J. Bacteriol. **173:**5315–5327.
38. **Zhou, N. Y., A. Jenkins, C. K. Chan Kwo Chion, and D. J. Leak.** 1998. The alkene monooxygenase from Xanthobacter Py2 is a binuclear non-haem iron protein closely related to toluene 4-monooxygenase. FEBS Lett. **430:**181–185.